Ecotoxicology and Environmental Safety 215 (2021) 112159

Contents lists available at ScienceDirect

Ecotoxicology and Environmental Safety

journal homepage: www.elsevier.com/locate/ecoenv

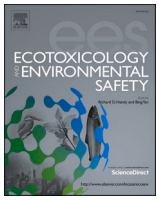

Immobilization properties and adsorption mechanism of nickel(II) in soil by biochar combined with humic acid-wood vinegar

Junfeng Zhu [a,b,*], Weichun Gao [b], Lei Ge [a], Wentian Zhao [b], Guanghua Zhang [b], Yuhua Niu [b]

[a] Key Laboratory of Degraded and Unused Land Consolidation Engineering, the Ministry of Natural Resources of the People's Republic of China, 710075, China
[b] Shaanxi Key Research Laboratory of Chemical Additives, College of Chemistry and Chemical Engineering, Shaanxi University of Science & Technology, Xi'an 710021, China

ARTICLE INFO

Edited by Dr. R. Pereira

Keywords:
Metal contaminated soil
Humic acid
Wood vinegar
Adsorption mechanism
Remediation performance

ABSTRACT

Biochar (BC) combined with humic acid (HA) and wood vinegar (WV) was designed and prepared as an inexpensive, effective, and environmentally friendly immobilization material (BHW) for metal-polluted soil. The influences of the wood vinegar and humic acid on the immobilization properties and adsorption mechanism of this new material were also investigated. The remediation performance was evaluated using a laboratory-made, nickel-contaminated soil with a Ni^{2+} concentration of 200 mg per kg surface soil (top 20 cm from agricultural land). The results indicated that the immobilization ratio sequence of nickel (II) in the soil was BC < BH < BHW. The maximum adsorption capacity increased in the same order: BC < BH < BHW. All three adsorption isotherms were better fitted by the Freundlich model, which were consistent with the surface heterogeneity of the remediation materials. The cause of this surface heterogeneous migration may be due to the increase in oxygen-containing groups in the BC introduced by the HA and WV. The WV can increase the number of the oxygen-containing groups in the BC combined with HA, which enhanced the adsorption and immobilization of Ni^{2+} ions. The results suggested that BHW is recommended for the remediation of metal-contaminated soils, because of its high efficacy, economic feasibility, environmental and food safety.

1. Introduction

Metal pollutants are introduced unintentionally to soil through human activities such as smelting, mining, irrigation, electronic industries, waste disposal, agrochemical use, war and military training, and consumption of fossil fuels (Liu et al., 2018a). Soil contamination by metals (such as lead (Pb), chromium (Cr), cadmium (Cd), copper (Cu), mercury (Hg), and nickel (Ni)) has been widely reported and is causing people to worry about the effects of the metals on living organisms, including humans (Palansooriya et al., 2020; Li et al., 2015; Wang et al., 2018a). Nickel is present in all soils and is derived from the parent material of lithogenic sources, artificial sediment, or both. At very low levels, Ni is an essential micronutrient, but at high levels, it can be toxic (Shahzad et al., 2018). The risk of ecotoxicity associated with nickel in the soil depends primarily on the living organisms (plants and animals) and the water resources which may have been exposed to nickel (Echevarria et al., 2006; Sun and Luo, 2018; Yeganeh et al., 2013). Due to the high nickel content in the soil, water, plants, and food, growing attention is being paid to its toxic effects (Yeganeh et al., 2013). With the increasing threat of contaminated soil to human health, it has become more and more important to identify and optimize soil remediation technologies.

Many soil remediation technologies have been used to reduce the risks associated with metal pollution and to recover degraded arable land for agricultural production and ensure food safety (Wang et al., 2015; Beiyuan et al., 2017; Li et al., 2018a). Various technologies are often used to diminish the bioavailability of metals present in soils. *Ex situ* techniques include soil washing, field irrigation, and bioreactors (Kuppusamy et al., 2016). *In situ* technologies include immobilization, stabilization, soil flushing, phytoremediation, and biological treatments (Benzon and Lee, 2017). Among these techniques, soil remediation methods for immobilizing metals have been widely used for the remediation of soils contaminated by metals due to their quick and easy application and commercial feasibility (Cao et al., 2019; Wang et al., 2018b). Selecting appropriate immobilizing materials can provide cost-effective remediation technologies and will implement the "green and sustainable remediation" principle (Hou and Altabbaa, 2014; Palansooriya et al., 2020). In general, studies on low-cost and

* Correspondence to: College of Chemistry and Chemical Engineering, Shaanxi University of Science & Technology, Xi'an 710021, China.
E-mail address: zjfeng123123@163.com (J. Zhu).

https://doi.org/10.1016/j.ecoenv.2021.112159
Received 18 April 2020; Received in revised form 5 March 2021; Accepted 14 March 2021
Available online 30 March 2021
0147-6513/© 2021 The Authors. Published by Elsevier Inc. This is an open access article under the CC BY-NC-ND license (http://creativecommons.org/licenses/by-nc-nd/4.0/).

environmentally-friendly materials for metal contaminated soil have received widespread attention in recent years (Palansooriya et al., 2020).

Great attention has been paid to waste recycling materials, furthermore, several materials have been suggested for soil reclamation, including biochar (BC) (Kuppusamy et al., 2016), humic substances (Piccolo et al., 2019), and wood vinegar (WV) (Liu et al., 2018b). The main mechanisms of biochar immobilization in soil involve alkalization, enhanced ion exchange capacity, and increased physical adsorption and precipitation (Li et al., 2017). The passivation effects of humic substances are usually ascribed to the formation of metal-humus complexes, as well as the existence of hydroxyl, carboxyl, and amino groups (Park et al., 2013). The ability of humic substances to bind metal ions can be ascribed to their high content of oxygen-containing functional groups, incorporating various types of carboxyl, hydroxyl, enol, phenol, and carbonyl structures (Pukalchik et al., 2018; Clemente and Bernal, 2006). Wood vinegar (WV) is a dark brown liquid, rich in organic acids obtained from the by-products during the carbonization of wood (Chen et al., 2016; Souza et al., 2012). The components of WV are associated with different kinds of organic compounds, which are mainly organic acids, phenols, and other compounds, such as aldehydes, alcohols, esters, ketones, furan and pyran derivatives, hydrocarbons, and nitrogen compounds (Li et al., 2018b; Lu et al., 2017). WV has been shown to reduce the concentrations of metal ions in soil and prevented their uptake through plant stabilization (Theapparat et al., 2015). WV-related humic substances inherently have adsorption sites available for metal chelation, reducing the bioavailability of metals (Lu et al., 2015; Benzon and Lee, 2017; Li et al., 2019). Recently, wood vinegar has been used to compost solid wastes (Liu et al., 2018b) and charcoal (Chen et al., 2010) to adsorb and immobilize metal contaminants, such as nickel, zinc, and copper. Wood vinegar can change the structure of organic matter during composting in the metal contaminated soil. The composted organic matter, such as humic acid substances, which are important organic matter in soil, can generate insoluble metal-organic compounds, thus lowering the amount of bioavailable metal in the soil (Liu et al., 2018b; Clemente and Bernal, 2006; Kulikowska et al., 2015). It was suggested that the conformational structure of humic acid was altered by small changes in ionic strength or pH value, which caused it to flocculate or aggregate (Clemente and Bernal, 2006; Zou et al., 2005). However, there is limited information on the influences of biochar combined with humic acid substances and wood vinegar, regarding the bioavailability of metals in contaminated soils. Therefore, this study focuses on investigating biochar combined with wood vinegar and humic acid as remediation materials to immobilize Ni^{2+} from contaminated soil. While creating new reuse options for waste materials such as WV, the remediation process can be low-cost and low impact.

This work extends a paradigm to an environmentally friendly active method for biochar combined with humic acid to immobilize metal ions in the metal-polluted soil. The design of the remediation material was optimized for maximizing the immobilization of Ni^{2+} from soil. To assess the influence of wood vinegar on the adsorption of metals by biochar combined with humic acid, the adsorption characterization of Ni^{2+} on the remediation material was investigated using Fourier-transform infrared spectroscopy (FT-IR). The mechanism of adsorbing and immobilizing metals from soil was studied by X-ray photoelectron spectroscopy (XPS). The microstructures before and after adsorbing Ni^{2+} were investigated using scanning electron microscopy/ energy-dispersive X-ray spectroscopy (SEM/EDS). The results will provide some insight for making an environmentally sustainable remediation material for metal-contaminated soil. At the same time, it also exploits a reasonable method for the re-utilization of industrial wastes and by-products.

2. Materials and methods

2.1. Materials and soil samples

Sodium humate for agriculture, which contained 52% humic acid, was a deep brown powder with a size of 0.075 mm (200 mesh), and was purchased from the Zibo Hongtong Chemical Co., Ltd (Zibo, China). Its water solubility was not less than 85% and had a pH value of 10.36. The wood vinegar was provided by the Jinan Xinyi Chemical Co., Ltd (Jinan, China). It was refined from a waste liquid produced by the manufacturing of charcoal using fruit shells and the specific gravity of the wood vinegar was 1.086 g mL^{-1}. The pH of the WV was 3.36–3.96. The biochar powder was obtained from the Tairan Group Co., Ltd (Guangrang, China). It was ground, sieved with a 0.28 mm (50 mesh) sieve, and dried at 105 °C for 12 h before use. Nickel nitrate hexahydrate (analytical reagent grade) was purchased from Shanghai Macklin Biochemical Co., Ltd (Shanghai, China). Hydrochloric acid (37%, analytical reagent grade) was purchased from Sinopharm Chemical Reagent Co., Ltd (Shanghai, China).

An artificially Ni-contaminated soil was used in this experiment. The superficial soil sample (0–20 cm) was taken from agricultural land in Xi'an, Shaanxi province, China. The soil samples were air-dried, crushed, and passed through a 0.125-mm sieve to remove impurities (stones, animal and plant remains) then homogenized and used as an original soil sample. 1 kg of the original soil sample was laboratory polluted using $Ni(NO_3)_2{\cdot}6H_2O$ aqueous solution (containing 201.3 mg/kg Ni^{2+}) to form a contaminated soil sample, according to the nickel-metal risk control standard (200 mg kg^{-1}) for soil contamination of agricultural land (GB15618-2018, China). The contaminated soil sample was aged for 30 days and used as the control soil sample (Peng et al., 2011). The physicochemical properties of experimental soil were: clay = 5.9%, silt = 48.3%, sand = 46.2%, pH = 6.5 ± 0.1, TOC = 4.20 ± 0.00%, CEC = 180 ± 3.2 mmol kg^{-1}, P_{tot} = 0.02 ± 0.00%, K_{tot} = 0.25 ± 0.00%, Mg_{tot} = 0.12 ± 0.00%, Ca_{tot} = 0.14 ± 0.01%. Nitot = 201.3 ± 18 mg kg.

2.2. Preparation of remediation materials

The biochar combined with humic acid and wood vinegar remediation materials were prepared by sodium humate, wood vinegar solution, and biochar powder with a mass ratio of 1:1:1.5 (Pukalchik et al., 2017). The material composition of each group is displayed in Table S1. Biochar powder (42.8 wt% of the remediation material) was mixed with sodium humate (28.6 wt%), crushed thoroughly, dried, and wood vinegar was added (28.6 wt%) (Pignatello et al., 2006). The mixture was air-dried to make particles and then sieved to obtain the humic acid-wood vinegar remediation material, BHW. As the control group, the BH group was composed of biochar powder (42.8 wt%) and sodium humate (57.2 wt %), while the BC group was composed of only biochar powder (100 wt %) under the same processing conditions.

2.3. Immobilization experiment

All remediation materials were completely mixed with the contaminated soil and allowed to react for 30 days (Kulikowska et. al, 2015). The six treatment groups of 0.04 g kg^{-1}, 0.1 g kg^{-1}, 0.2 g kg^{-1}, 0.3 g kg^{-1}, 0.4 g kg^{-1} and 0.5 g kg^{-1} were denoted as remediation materials BHW-1, BHW-2, BHW-3, BHW-4, BHW-5, and BHW-6, respectively. The same amounts of BH treatment groups were denoted as BH-1, BH-2, BH-3, BH-4, BH-5, and BH-6, respectively. Biochar treatment groups were respectively denoted as BC-1, BC-2, BC-3, BC-4, BC-5, and BC-6. The contaminated soil after aging without any remediation was used as a control group. Three replicated samples were prepared for each treatment group to ensure the accuracy of the data.

2.4. Immobilization determination of the remediation on Ni $^{2+}$

The amount of extracted nickel(II) was tested after 30 days of reaction in the same environment using a five-point sampling method. The extracted nickel(II) for the control and the treatment groups were removed with 0.1 mol L^{-1} HCl at 25 ± 2 °C and shaken for 2 h (Xu et al., 2013). Then, the extracted solutions were diluted to 100 mL using deionized water. After that, the diluted solutions were filtered through a 0.22 μm filter. The filtrates were analyzed by using a Z-2000 graphite furnace atomic absorption spectrometer (AAS) (HITACHI, Japan) to determine the amount of dissolved Ni in the solution. Three replicated samples were analyzed for each treatment and the average value of the extracted nickel(II) was reported. The immobilization ratio of nickel(II) in the soil was defined as:

$$\text{Immobilization ratio } (\%) = (c_1 - c_2)/c_1 \times 100\% \quad (1)$$

where c_1 represents the nickel(II) concentration in the contaminated soil before the remediation treatment (mg kg^{-1}) and c_2 represents the nickel (II) concentration in the contaminated soil after remediation (mg kg^{-1}).

2.5. Sorption of remediation materials

Experiments for Ni adsorption were performed by a batch method. 0.5 g of either the BC, the BH, or the BHW remediation material were respectively added into 100 mL polyethylene centrifuge tubes. Then the tubes were added by 40 mL Ni^{2+} solutions with a serial of concentration from 0 mg L^{-1} to 300 mg L^{-1} (0.01 mol L^{-1} $NaNO_3$ as the background of the Ni solutions). After that, the adsorption processes of the remediation material in the solutions were carried out for 24 h at 25 °C in a constant temperature shaker controller (Miao et al., 2011). When the adsorption process was completed, the sample was quickly filtered through a 0.22 μm membrane and the residual Ni^{2+} concentration in the filtrate was analyzed. Adsorption isotherms with initial concentrations of Ni^{2+} in the range of 0 mg L^{-1} to 300 mg L^{-1} were also studied. Three replicated samples were carried out for the sorption experiments.

2.6. Determination of adsorption/immobilization mechanism

All samples of BC, BH, and BHW before and after Ni^{2+} absorption were washed three times with ultrapure water to remove any physisorbed Ni^{2+} and dried under vacuum overnight before all tests (Tian et al., 2012). A VECTOR-22 FT-IR spectrometer (Bruker, Germany) was utilized to obtain the FT-IR spectra of the samples with the potassium bromide disc technique (Wu et al., 2020). A Q45 SEM (FEI, USA) was used to characterize the micromorphology of the material. The samples were fixed on the conductive adhesive. After being sprayed with gold, the samples were fixed on the sample table and tested at a magnification of 20,000 (Zeng et al., 2021). XPS analysis was conducted using an AXIS Supra type XPS spectrometer (Kratos, UK). The measurement spectrum was obtained over the range of 0–1200 eV, with an energy of 300 eV and a slit width of 1.9 mm into the analyzer. The binding energy was calibrated with taking the C 1s peak as 284.60 eV (Nesbitt et al., 2000; Tan et al., 2008). All of the analyses were conducted in duplicate.

2.7. Statistical analysis

Two-way analysis of variance (ANOVA) was performed to analyze the data of extractable nickel(II) at $P < 0.05$ using SPSS Statistic 22 (Analytical software, United States). The means and standard deviations (SD) of Ni extraction techniques were estimated using Microsoft Excel (2018) while the figures were visualized using Origin 8.5 software (OriginLab, United States). Each treatment had three replicates.

3. Results and discussion

3.1. Optimal remediation material and dosage for immobilization of Ni (II)

The results of the extractable Ni experiments to determine the optimal remediation material and treatment dosage are shown in Fig. 1. The control group represents contaminated soil after aging without any remediation. Fig. 1a shows the influence of the three remediation groups and various dosages on the amount of extractable Ni. The amount of extractable Ni was significantly decreased by the incorporation of each remediation material. For the different treatment effects, the mean extractable Ni of the BHW treatment group was significantly lower than in the other treatment groups. The trend of the amounts of extractable Ni in the remediation soil, in a descending order was BC > BH > BHW. This order of extractable Ni in soils agrees with previous studies (Chen et al., 2010; Basu et al., 2019). For the treatment dose effect, the trend of the three remediation groups was expanded. The trend amounts of extractable Ni were very similar at the same dosage.

In order to explore the immobilization property of the three treatment groups, the immobilization ratios of nickel(II) in the soil were shown in Fig. 1b. It indicated that BHW presented the best immobilization efficiency for Ni^{2+}. The BHW treatment dosage was 0.1 g kg^{-1}, which significantly reduced the Ni^{2+} present in the soil, and the immobilization ratio was as high as 60.1%. This result was better than Ni immobilization (35.4–46.1%) in the reference report (Kulikowska et al., 2015). At the same dosage (0.1 g kg^{-1}), the Ni^{2+} immobilization ratio of the BHW treatment was 18.5% higher than BH. The immobilization ratio of nickel(II) for the BHW treatment was increased by at least 23.1% compared to the unmodified biochar. The percentage of Ni^{2+} in the water was decreased when the amount of the remediation material was greater than 0.1 g kg^{-1}. This may be related to the dissolved organic carbon (DOC) in the soil because the addition of WV improves the DOC. High DOC in soil facilitates the formation of soluble metal complexes, thus increasing metal mobility (Palansooriya et al., 2020). This indicated that the addition of wood vinegar enhanced Ni^{2+} sorption on the humic acid and is economically feasible. BHW has a better effect on Ni^{2+} immobilization in the soil at a lower treatment dosage than the other remediation materials.

3.2. Adsorption capacity of Ni^{2+} on BC, BH, or BHW

To evaluate the Ni adsorption capacities of BC, BH, or BHW, the adsorption isotherms of Ni^{2+} on BC, BH, and BHW were investigated and are shown in Fig. 2a. The two most widely used isotherm models, Freundlich and Langmuir, were chosen to model the adsorption of Ni^{2+} on BH and BHW (Zhang et al., 2015; Doulia et al., 2009). The Freundlich isotherm is an empirical equation that assumes multiple layers of adsorption onto a heterogeneous surface which is composed of different types of adsorption sites. Therefore, infinite surface coverage can be predicted, mathematically, which indicates multi-layer adsorption on the surface. The Langmuir isotherm stems from the assumption that all adsorption sites are identical and that the adsorption on the active sites is independent of whether or not adjacent sites are occupied. Table 1 lists the simulated isotherm parameters and correlation coefficients (R^2). Comparing the R^2 values of the two isotherm models, it was found that the Freundlich model (R^2 = 0.993–0.997) has a better fit than the Langmuir model (R^2 = 0.973–0.982). According to literature, (Zhang et al., 2015; Liu et al., 2018b) the results imply that the Ni(II) was probably adsorbed on the surface of BC, BH, or BHW in both monolayers and multilayers. The maximum sorption amounts of Ni(II) on BH (12.78 mg/g) was obtained by the Langmuir model was very close to a previous report (12.41 mg/g), however, the maximum amounts of adsorption on BHW (16.32 mg/g) was larger than that of a previous report (Basu et al., 2019). The results indicated that WV can enhance the adsorption of Ni(II) to BH. The form of the Freundlich equation is:

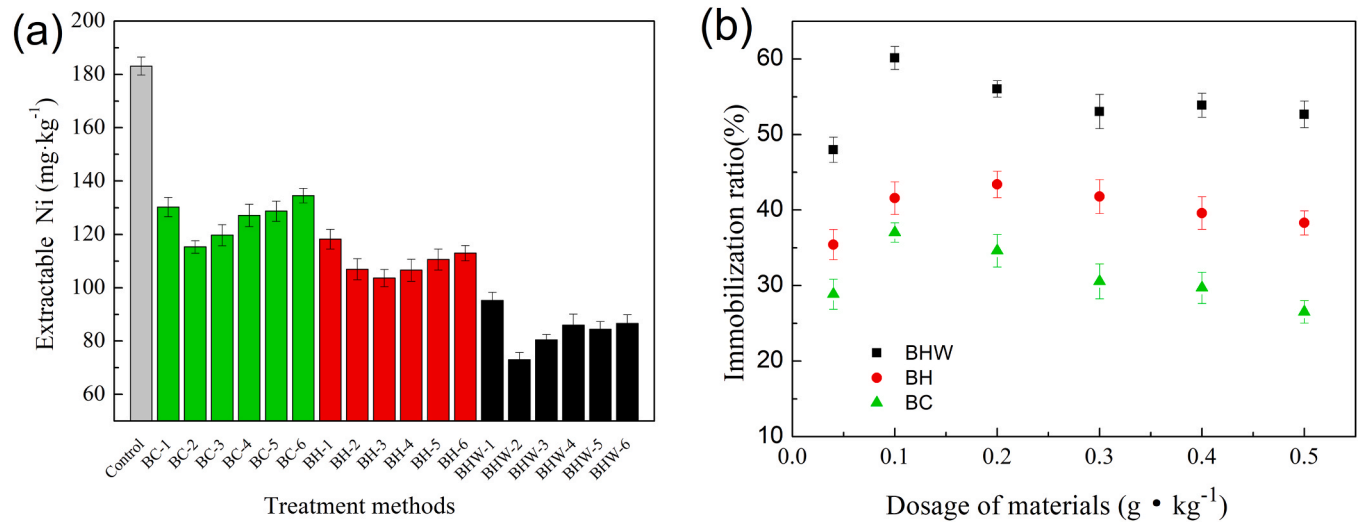

Fig. 1. (a) The extractable Ni from the control and all treatment groups. The control group represents contaminated soil after aging without any remediation; (b) Soil Ni^{2+} immobilization ratios of all treatment groups according to the mean value of extractable Ni (mean ± SD) at $P < 0.05$ ($n = 3$).

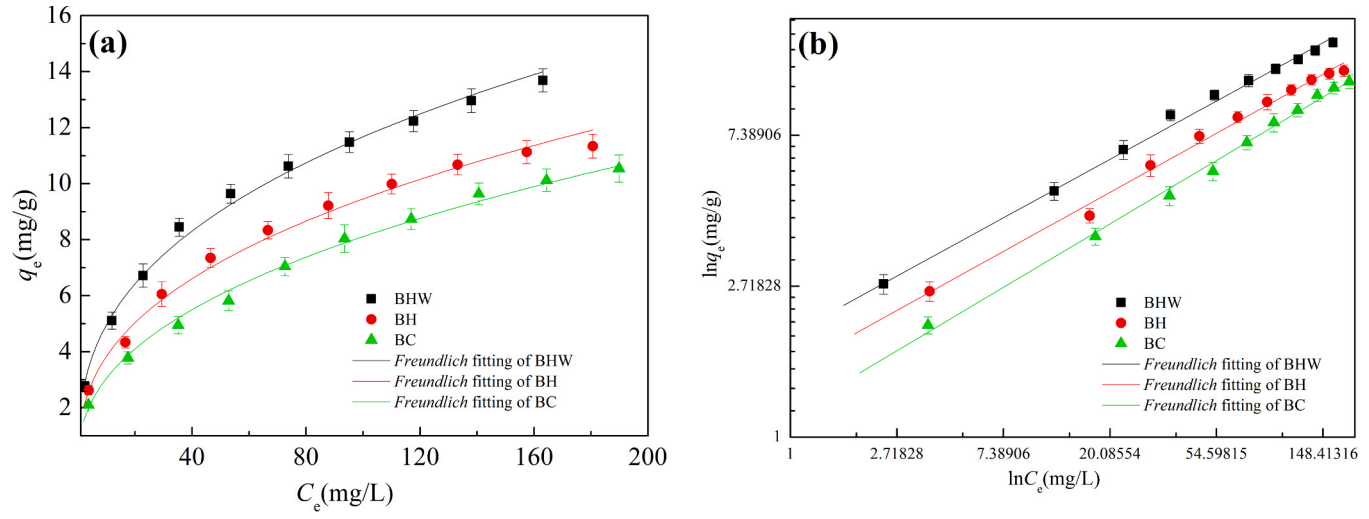

Fig. 2. The adsorption isotherms (a) and linear form (b) of Ni^{2+} on BHW, BH, and BC at the temperature of 25 °C.

Table 1
Fitting parameters of Freundlich and Langmuir isotherm for the adsorption of Ni^{2+} onto BC, BH and BHW[a].

Remediation materials	Langmuir			Freundlich		
	q_m (mg/g)	k_L (L/mg)	R^2	k_F	1/n	R^2
BC	11.24	0.043	0.982	1.15	0.42	0.997
BH	12.78	0.050	0.973	1.56	0.39	0.993
BHW	16.32	0.055	0.979	2.12	0.37	0.996

[a] Three replicated samples were carried out for the sorption experiments and the mean values were presented.

$$q_e = k_F C_e^{1/n} \quad (2)$$

This equation can also be expressed in a linear form as:

$$\ln q_e = \ln k_F + 1/n \ln C_e \quad (3)$$

where q_e is the adsorbed amount of Ni^{2+} per unit weight of remediation material (mg/g), C_e is the equilibrium concentration of Ni^{2+} in solution (mg/L), and k_F is a measure of the adsorption capacity. According to the values of k_F, BHW had a high adsorption capacity for Ni^{2+} because it coexisted with WV and HA. The 1/n of the Freundlich linear equation ranged between 0 and 1 and is a dimensionless parameter related to surface heterogeneity. A value of 1/n closer to 0 represented a more heterogeneous surface. Table 1 indicates that the value of 1/n (0−1) was a measure of the exchange intensity or surface heterogeneity, with a value of 1/n smaller than 1 describing favorable removal conditions (Li et al., 2019). Furthermore, 1/n was decreased in the order of BC > BH > BHW, which was indicative of an alteration toward a more heterogeneous surface (Zhang et al., 2015).

Fig. 2b shows the amount of Ni^{2+} adsorbed per unit weight of remediation material increased in the order of BC < BH < BHW, which was consistent with the surface heterogeneity of the remediation material (Liu et al., 2018b). The cause of the surface heterogeneous migration may be due to the increase in the number of oxygen-containing groups introduced by WV and HA, which led to the increase of high-energy adsorption sites and ultimately, the increase of surface adsorption of Ni^{2+}. The adsorption isotherms of Ni^{2+} on BHW show that the adsorption amounts of Ni^{2+} on BHW materials increased with increasing concentration of Ni^{2+}, therefore BHW can be used in Ni-polluted soil with a wide concentration range.

3.3. Adsorption mechanism

3.3.1. FT-IR of BH and BHW before and after Ni^{2+} adsorption

FT-IR spectra were taken to obtain information on the surface functional groups of BH and BHW before and after adsorbing Ni^{2+}. The FT-IR spectra are shown in Fig. 3. The peaks in the BH spectra were ascribed as follows: 3107 cm^{-1} was attributed to the stretching vibrations of hydroxyl groups and 1712 cm^{-1} was due to C=O stretching vibrations (Rodríguez et al., 2016). The peak at 1576 cm^{-1} was due to aromatic C=C and C=O stretching vibrations (Basu et. al, 2019). Peaks at 1106 cm^{-1} and 1021 cm^{-1} were associated with the stretching vibrations of C-O in an ether and an alcohol, respectively (Yang and Hodson, 2019). The C=O peak, together with peaks for C-O and C-OH also suggested the presence of a carboxyl functional group (O-C=O) (Liu et al., 2018b). This indicated that BH was rich in oxygen-containing groups. There were some changes in the wavenumbers and peak intensities of the FT-IR spectrum for BH after Ni^{2+}adsorption (HA-Ni), such as peaks centered at 1712 cm^{-1} and 1576 cm^{-1} moved to 1706 cm^{-1} and 1563 cm^{-1}, respectively. The peaks from O-H (3107 cm^{-1}), C=O (1712 cm^{-1}), and C-O (1106 cm^{-1}) became weaker than before adsorption, which revealed that the nickel (II) was binding with these groups.

The FT-IR spectrum of BHW (Fig. 3) also presented the same characteristic peaks as BH. However, the wavenumbers and intensities of the BHW characteristic absorption peaks had changed, such as the carboxyl group (O-C=O) and the hydroxyl group (C-OH) were significantly enhanced, which assisted the Ni^{2+} binding with these groups (Liu et al., 2018b). The FT-IR spectrum of BHW after Ni^{2+} adsorption (BHW-Ni) presented some definite changes in wavenumbers and peak intensities, such as the peaks of the carboxyl and hydroxyl groups. The interaction of BHW with Ni^{2+} was mainly the reaction with the hydroxyl and carboxyl groups in BHW (Tan et al., 2008). FT-IR verified that Ni^{2+} ions were immobilized through a complex reaction with the BHW remediation materials.

3.3.2. XPS analysis of BH and BHW adsorbing Ni^{2+}

XPS was performed to further determine the adsorption interaction between the BH and BHW remediation materials combined with Ni^{2+}. The survey spectra of BHW before and after adsorbing Ni^{2+} are respectively shown in Fig. 4. The characteristic Ni 2p photoelectron peaks are presented on the spectrum of BHW combined with Ni^{2+}, and corresponded to characteristic Ni 2p photoelectron peaks (Nesbitt et al., 2000). The Na 1s, Na KLL, Ca 2s, and Ca 2p spectra of BHW disappeared in the BHW-Ni spectrum. This suggested Ni^{2+} replaced Na^{+} and Ca^{2+} to complex with the oxygen-containing functional groups of BHW through ion exchange.

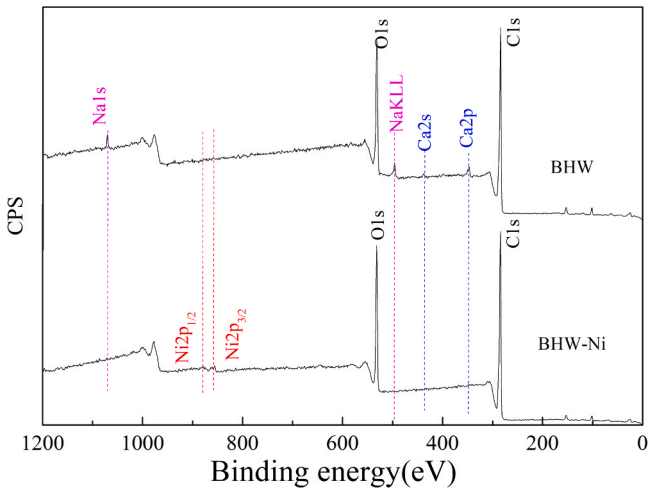

Fig. 4. XPS survey spectra of BHW and BHW-Ni.

To further analyze changes in binding energy between BH or BHW before and after adsorbing Ni^{2+}, the C 1s region of the XPS spectra of BHW, BH, and BC before and after adsorbing Ni^{2+} were respectively measured and are shown in Fig. 5(a) and (b). According to the relevant literature (Zhang et al., 2015; Bhargava et al., 2007), the C 1s spectra of BHW, BH, and BC all have the characteristics of three binding energy peaks at 284.60, 286.10, and 288.65 eV, which represent C=C/C-C, C-O, and O-C=O, respectively. As presented in Fig. 5(a), there are some differences between the C 1s peaks for BC, BH, and BHW. The significant differences in intensities were observed for peaks of the functional groups including C=C or C-C, C-O, and O-C=O (Chen et al., 2020). The content of the oxygen incorporating functional groups, such as C-O and O-C=O, observably increased in the order of BC < BH < BHW. From the comparison of Fig. 5(a) and (b), there were some differences between

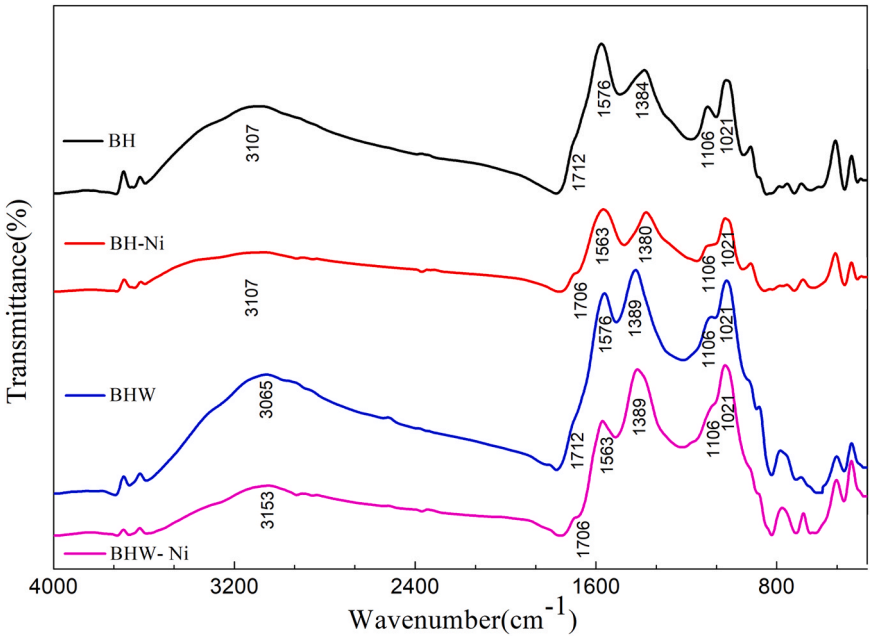

Fig. 3. FT-IR comparison before and after Ni^{2+} adsorption by BH and BHW.

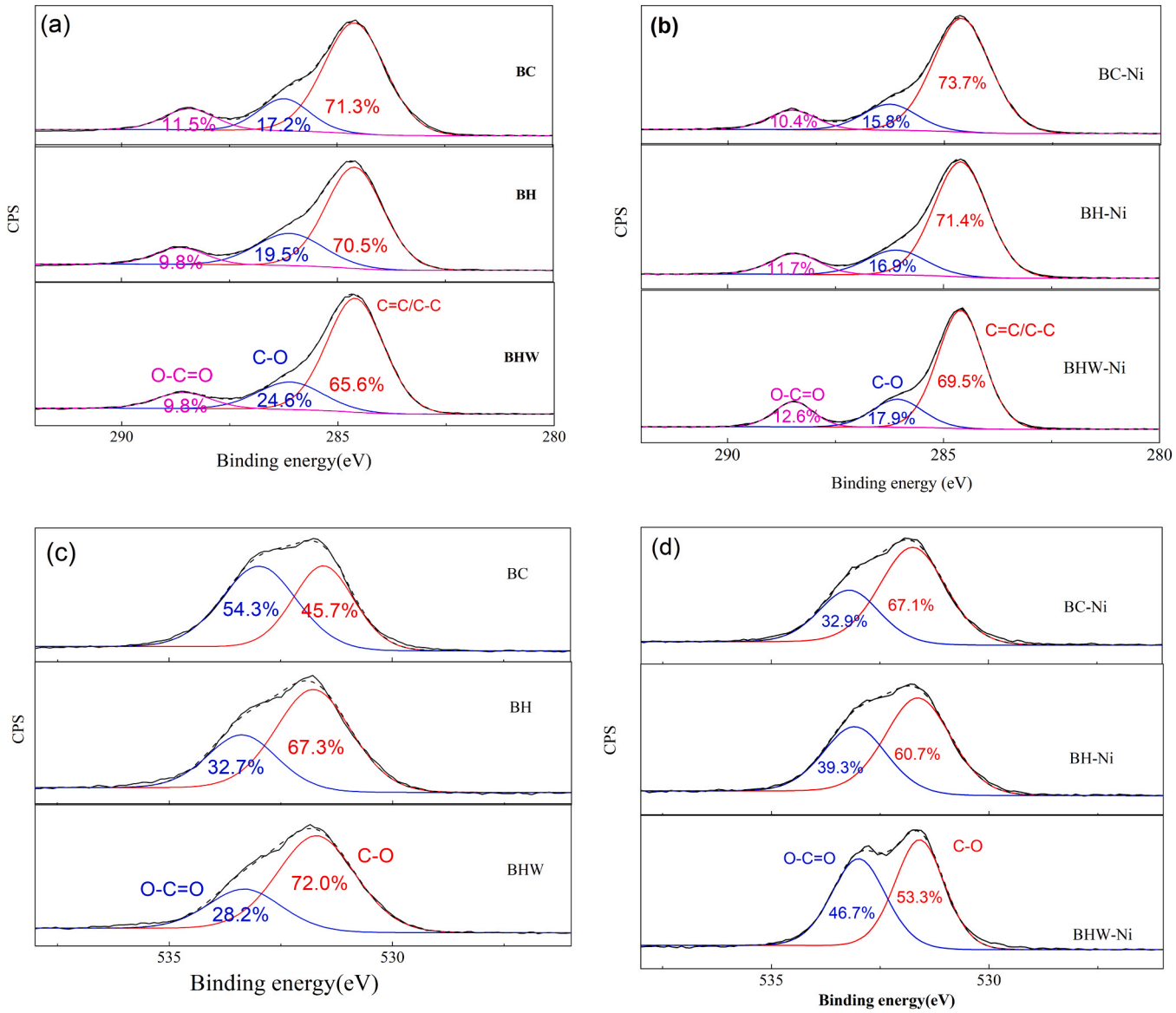

Fig. 5. The XPS spectra of C 1s (a, b) and O 1s (c, d) for BC, BH, BHW, BC-Ni, BH-Ni, and BHW-Ni.

the C 1s peaks for BC, BH, and BHW before and after the adsorption of Ni^{2+} ions. The content of oxygen-containing functional groups decreased after the adsorption of Ni^{2+} ions. These main differences verified that oxygen functional groups formed complexes with Ni^{2+} ions.

The O 1s region of the BC, BH, and BHW XPS spectra before and after adsorbing Ni^{2+} were measured and are shown in Fig. 5(c) and (d). According to the relevant literature (Vieira et al., 2011), the O 1s spectra of BHW, BH, and BC have the characteristics of two binding energy peaks at 531.70 and 533.31 eV, which were attributed to C-O and O-C=O, respectively. Fig. 5(c) shows that the content of C-O functional groups dramatically increased in the order of BC < BH < BHW. It may be due to the fact that BC covered by HA and WV improved the proportion of C-O functional groups on the BC. Comparing Fig. 5(c) and (d), it was observed that the content of C-O decreased after adsorption of the Ni^{2+} ions. This was also verified by the IR results, that is, the interaction between BHW, BH, and Ni^{2+} was mainly with the hydroxyl and carboxylic acid groups in BHW. These results of the significant differences of functional groups indicate that Ni(II) was adsorbed on the surface functional groups of BHW by chemical complexation (forming Ni(II)-HA complexes), electrostatic attraction, or cation exchange, which occurred between Ni(II) and the surface functional groups of BHW and surface-bound HA.

3.3.3. *SEM/EDS of BH and BHW before and after Ni^{2+} adsorption*

SEM and EDS analysis were performed to gain more insights into the adsorption mechanism. SEM images and EDS diagrams of the BH and BHW and their combination with Ni^{2+} are displayed in Fig. 6. Based on samples of BH and BHW, which were magnified 4000 times, the characteristic irregular surfaces of the BC were found from these micrographs. However, some changes in the characteristic surface of the BC took place in BH and BHW. A significant change in the surface could be illustrated by the fact that the surface of the BC was partly covered by HA or HA and WV. Compared with BH, the BHW presented a more heterogeneous surface. This benefitted the adsorption reaction with Ni^{2+}, according to the adsorption section results. The EDS spectra showed that the content of nickel in BHW-Ni was larger than in BH-Ni, which was caused by the fact that there were more oxygen-containing groups in BHW than BH for Ni^{2+} to form complexes with. This was closely consistent with the FT-IR results. It also confirmed the previous adsorption section result that the surface heterogeneous shift was caused by the HA and WV, which can enhance adsorption capabilities. Besides, the contents of some metal ions, such as Na^{+}, Ca^{2+}, Mg^{2+}, and Al^{3+}, also

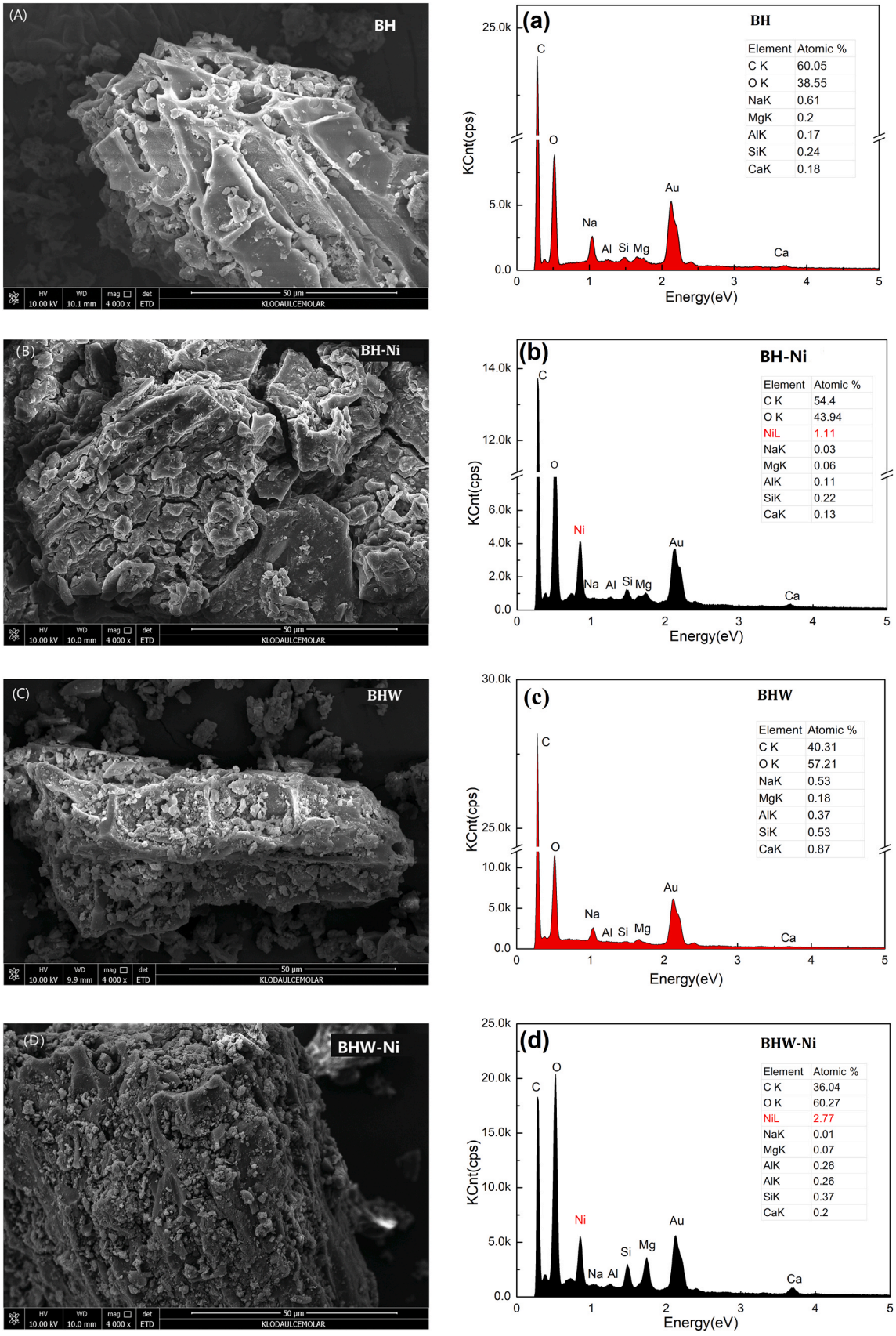

Fig. 6. SEM images (magnified 4000 times) of (A) BH, (B) BH-Ni, (C) BHW, (D) BHW-Ni, and their EDS diagrams of (a) BH, (b) BH-Ni, (c) BHW, (d) BHW-Ni.

notably changed after the Ni^{2+} adsorption, which indicated that BH and BHW have ion exchange with the contaminated soil. For the BHW remediation material, the organic substances associated with WV were made with numerous adsorption sites for chelation, rendering metals less available for uptake. Wood vinegar can change the amount of the oxygen-containing functional groups present on the humic substances during composting in the metal-contaminated soil (Liu et al., 2018b). The composted humic substances can then form insoluble metal-organic compounds, thus reducing the amount of bioavailable metal in the soil.

4. Conclusions

Biochar combined with humic acid and wood vinegar (BHW) was created and evaluated as a new type of inexpensive, effective, and environmentally friendly immobilization material for metals in soil. Application experiments showed that the immobilization ratio of Ni^{2+} was up to 60.10 wt% when 0.1 g BHW was added per kg of the top 20 cm of surface soil. The BHW not only has physisorption and precipitation from BC, but also chemical complexation or sorption from HA and WV. Wood vinegar can activate humic acid to promote the increase of oxygen-containing functional groups, incorporating carboxyl and hydroxyl groups which subsequently enhance the adsorption and immobilization of Ni^{2+} in the soil. Adsorption isotherms and SEM/EDS analysis show that BHW had a more heterogeneous surface to adsorb more Ni^{2+} than BC or BH. XPS indicated that there was a Ni 2p spectrum in BHW, which was combined with Ni^{2+} by chemical adsorption, mainly by an oxygen-containing functional group reaction. Finally, it is suggested that biochar combined with humic acid and wood vinegar can be a good option for immobilizing nickel in contaminated soils.

CRediT authorship contribution statement

Junfeng Zhu: Conceptualization, Project administration, Writing - reviewing & editing, Formal analysis. **Weichun Gao**: Visualization, Data curation. **Lei Ge**: Investigation. **Wentian Zhao**: Writing - original draft. **Guanghua Zhang**: Methodology. **Yuhua Niu**: Resources.

Declaration of Competing Interest

The authors declare that they have no known competing financial interests or personal relationships that could have appeared to influence the work reported in this paper.

Acknowledgements

This work was granted by Key Laboratory of Degraded and Unused Land Consolidation Engineering, the Ministry of Natural Resources of the People's Republic of China (Grant No. SXDJ2018-01), Shaanxi Province Science and Technology Project (Grant No. 2021SF-431 and S2020-YF-YBNY-0235), and Xi'an Science and Technology Plan Project (Grant No. 201805023 YD1CG7(3) and 20SFSF0016).

Appendix A. Supporting information

Supplementary data associated with this article can be found in the online version at doi:10.1016/j.ecoenv.2021.112159.

References

Basu, H., Saha, S., Mahadevan, I.A., Pimple, M.V., Singhal, R.K., 2019. Humic acid coated cellulose derived from rice husk: a novel biosorbent for the removal of Ni and Cr. J. Water Process Eng. 32, 100892.
Beiyuan, J., Li, J.S., Tsang, D.C.W., Wang, L., Poon, C.S., Li, X.D., Fendorf, S., 2017. Fate of arsenic before and after chemical-enhanced washing of an arsenic-containing soil in Hong Kong. Sci. Total Environ. 599–600, 679–688.
Benzon, H.R.L., Lee, S.C., 2017. Pyroligneous acids enhance phytoremediation of heavy metal-contaminated soils using mustard. Commun. Soil Sci. Plant Anal. 48 (5), 1–13.
Bhargava, G., Gouzman, I., Chun, C.M., Ramanarayanan, T.A., Bernasek, S.L., 2007. Characterization of the "native" surface thin film on pure polycrystalline iron: a high resolution XPS and TEM study. Appl. Surf. Sci. 253 (9), 4322–4329.
Cao, X., Wang, W., Ma, R., Sun, S., Lin, J., 2019. Solidification/stabilization of Pb2+ and Zn2+ in the sludge incineration residue-based magnesium potassium phosphate cement: physical and chemical mechanisms and competition between coexisting ions. Environ. Pollut. 253, 171–180.
Chen, H., Li, Q., Wang, M., Ji, D., Tan, W., 2020. XPS and two-dimensional FTIR correlation analysis on the binding characteristics of humic acid onto kaolinite surface. Sci. Total Environ. 724, 138154.
Chen, J., Wu, J.H., Si, H.P., Lin, K.Y., 2016. Effects of adding wood vinegar to nutrient solution on the growth, photosynthesis, and absorption of mineral elements of hydroponic lettuce. J. Plant Nutr. 39 (4), 456–462.
Chen, Y.X., Huang, X.D., Han, Z.Y., Huang, X., Hu, B., Shi, D.Z., Wu, W.X., 2010. Effects of bamboo charcoal and bamboo vinegar on nitrogen conservation and heavy metals immobility during pig manure composting. Chemosphere 78 (9), 1177–1181.
Clemente, R., Bernal, M.P., 2006. Fractionation of heavy metals and distribution of organic carbon in two contaminated soils amended with humic acids. Chemosphere 64 (8), 1264–1273.
Doulia, D., Leodopoulos, C., Gimouhopoulos, K., Rigas, F., 2009. Adsorption of humic acid on acid-activated Greek bentonite. J. Colloid Interface Sci. 340 (2), 131–141.
Echevarria, G., Massoura, S.T., Sterckeman, T., Becquer, T., Schwartz, C., Morel, J.L., 2006. Assessment and control of the bioavailability of nickel in soils. Environ. Toxicol. Chem. 25 (3), 643–651.
Hou, D., Altabbaa, A., 2014. Sustainability: a new imperative in contaminated land remediation. Environ. Sci. Policy 39, 25–34.
Kulikowska, D., Gusiatin, Z.M., Bułkowska, K., Klik, B., 2015. Feasibility of using humic substances from compost to remove heavy metals (Cd, Cu, Ni, Pb, Zn) from contaminated soil aged for different periods of time. J. Hazard. Mater. 300, 882–891.
Kuppusamy, S., Thavamani, P., Megharaj, M., Venkateswarlu, K., Naidu, R., 2016. Agronomic and remedial benefits and risks of applying biochar to soil: current knowledge and future research directions. Environ. Int. 87, 1–12.
Li, H., Dong, X., Da Silva, E.B., De Oliveira, L.M., Chen, Y., Ma, L.Q., 2017. Mechanisms of metal sorption by biochars: biochar characteristics and modifications. Chemosphere 178, 466–478.
Li, J.S., Wang, L., Cui, J.L., Poon, C.S., Beiyuan, J., Tsang, D.C., Li, X.D., 2018a. Effects of low-alkalinity binders on stabilization/solidifcation of geogenic As-containing soils: spectroscopic investigation and leaching tests. Sci. Total Environ. 631, 1486–1494.
Li, N., Kang, Y., Pan, W., Zeng, L., Zhang, Q., Luo, J., 2015. Concentration and transportation of heavy metals in vegetables and risk assessment of human exposure to bioaccessible heavy metals in soil near a waste-incinerator site, South China. Sci. Total Environ. 521–522, 144–151.
Li, Z., Wu, L., Sun, S., Gao, J., Zhang, H., Zhang, Z., Wang, Z., 2019. Disinfection and removal performance for Escherichia coli, toxic heavy metals and arsenic by wood vinegar-modified zeolite. Ecotoxicol. Environ. Saf. 174, 129–136.
Li, Z., Zhang, L., Chen, G., Wu, L., Liu, B., Li, Y., Sun, S., Zhang, H., Zhang, Z., Wang, Z., 2018b. A new method for comprehensive utilization of wood vinegar by distillation and liquid-liquid extraction. Process Biochem. 75, 194–201.
Liu, L., Guo, X., Wang, S., Li, L., Zeng, Y., Liu, G., 2018a. Effects of wood vinegar on properties and mechanism of heavy metal competitive adsorption on secondary fermentation based composts. Ecotoxicol. Environ. Saf. 150, 270–279.
Liu, L., Li, W., Song, W., Guo, M., 2018b. Remediation techniques for heavy metal-contaminated soils: principles and applicability. Sci. Total Environ. 633, 206–219.
Lu, H., Lashari, M.S., Liu, X., Ji, H., Li, L., Zheng, J., Kibue, G.W., Joseph, S., Pan, G., 2015. Changes in soil microbial community structure and enzyme activity with amendment of biochar-manure compost and pyroligneous solution in a saline soil from Central China. Eur. J. Soil Biol. 70, 67–76.
Lu, X.C., Jiang, J.C., Sun, Y.J., 2017. Review on preparation and application of wood vinegar. Chem. Ind. For. Prod. 37 (03), 21–30 (in Chinese).
Miao, Z., Wang, L., Ma, S., Wang, D., Zhang, Y., Li, Z., 2011. Novel functional material of starch microsphere and the adsorption properties for divalent nickel. J. Inorg. Organomet. Polym. Mater. 21 (4), 832–835.
Nesbitt, H.W., Legrand, D., Bancroft, G.M., 2000. Interpretation of Ni2p XPS spectra of Ni conductors and Ni insulators. Phys. Chem. Miner. 27 (5), 357–366.
Palansooriya, K.N., Shaheen, S.M., Chen, S.S., Tsang, D.C., Hashimoto, Y., Hou, D., Bolan, N.S., Rinklebe, J., Ok, Y.S., 2020. Soil amendments for immobilization of potentially toxic elements in contaminated soils: a critical review. Environ. Int. 134, 105046.
Park, S., Kim, K.S., Kang, D., Yoon, H., Sung, K., 2013. Effects of humic acid on heavy metal uptake by herbaceous plants in soils simultaneously contaminated by petroleum hydrocarbons. Environ. Earth Sci. 68, 2375–2384.
Peng, L.C., Huang, Z.B., Shi, Y., Sun, H.J., Shen, C., Chen, W., Zhang, X.M., 2011. Effects of environmental materials on maize growth and soil remediation of Pb and Cd contaminated soils. Chin. J. Eco Agric. 19 (6), 1386–1392 (in Chinese).
Piccolo, A., Spaccini, R., De Martino, A., Scognamiglio, F., Meo, V.D., 2019. Soil washing with solutions of humic substances from manure compost removes heavy metal contaminants as a function of humic molecular composition. Chemosphere 225, 150–156.
Pignatello, J.J., Kwon, S., Lu, Y., 2006. Effect of natural organic substances on the surface and adsorptive properties of environmental black carbon (char): attenuation of surface activity by humic and fulvic acids. Environ. Sci. Technol. 40 (24), 7757–7763.
Pukalchik, M., Mercl, F., Panova, M., Břendová, K., Terekhova, V.A., Tlustoš, P., 2017. The improvement of multi-contaminated sandy loam soil chemical and biological properties by the biochar, wood ash, and humic substances amendments. Environ. Pollut. 229, 516–524.

Pukalchik, M., Mercl, F., Terekhova, V., Tlustoš, P., 2018. Biochar, wood ash and humic substances mitigating trace elements stress in contaminated sandy loam soil: evidence from an integrative approach. Chemosphere 203, 228–238.
Rodríguez, F.J., Schlenger, P., García-Valverde, M., 2016. Monitoring changes in the structure and properties of humic substances following ozonation using UV–Vis, FTIR and ^{1}H NMR techniques. Sci. Total Environ. 541, 623–637.
Shahzad, B., Tanveer, M., Rehman, A., Cheema, S.A., Fahad, S., Rehman, S., Sharma, A., 2018. Nickel; whether toxic or essential for plants and environment - a review. Plant Physiol. Biochem. 132, 641–651.
Souza, J.B.G., Ré-Poppi, N., Raposo Jr., J.L., 2012. Characterization of pyroligneous acid used in agriculture by gas chromatography-mass spectrometry. J. Braz. Chem. Soc. 23 (4), 610–617.
Sun, X.J., Luo, H., 2018. Study on the characteristics and treatment of heavy metal pollution in soil. China Resour. Compr. Util. 36 (04), 144–151 (in Chinese).
Tan, X.L., Chang, P.P., Fan, Q.H., Zhou, X., Yu, S.M., Wu, W.S., Wang, X.K., 2008. Sorption of Pb (II) on Na-rectorite: effects of pH, ionic strength, temperature, soil humic acid and fulvic acid. Colloid Surf. A 328 (1–3), 8–14.
Theapparat, Y., Chandumpai, A., Leelasuphakul, W., Laemsak, N., 2015. Pyroligneous acids from carbonisation of wood and bamboo: their components and antifungal activity. J. Trop. For. Sci. 27 (4), 517–526.
Tian, X., Li, T., Yang, K., Xu, Y., Lu, H., Lin, D., 2012. Effect of humic acids on physicochemical property and Cd (II) sorption of multiwalled carbon nanotubes. Chemosphere 89 (11), 1316–1322.
Vieira, R.S., Oliveira, M.L.M., Guibal, E., Rodríguez-Castellón, E., Beppu, M.M., 2011. Copper, mercury and chromium adsorption on natural and crosslinked chitosan films: an XPS investigation of mechanism. Colloid Surf. A 374 (1–3), 108–114.
Wang, L., Chen, S.S., Sun, Y., Tsang, D.C., Yip, A.C., Ding, S., Hou, D., Baek, K., Ok, Y.S., 2018a. Efcacy and limitations of low-cost adsorbents for in-situ stabilisation of contaminated marine sediment. J. Clean. Prod. 212, 420–427.
Wang, L., Kwok, J.S., Tsang, D.C., Poon, C.S., 2015. Mixture design and treatment methods for recycling contaminated sediment. J. Hazard. Mater. 283, 623–632.
Wang, L., Yu, K., Li, J.S., Tsang, D.C., Poon, C.S., Yoo, J.C., Baek, K., Ding, S., Hou, D., Dai, J.G., 2018b. Low-carbon and low-alkalinity stabilization/solidification of high Pb contaminated soil. Chem. Eng. J. 351, 418–427.
Wu, M., Chen, Y., Lin, H., Zhao, L., Shen, L., Li, R., Xu, Y., Hong, H., He, Y., 2020. Membrane fouling caused by biological foams in a submerged membrane bioreactor: mechanism insights. Water Res. 181, 115932.
Xu, D., Zhou, P., Zhan, J., Gao, Y., Dou, C., Sun, Q., 2013. Assessment of trace metal bioavailability in garden soils and health risks via consumption of vegetables in the vicinity of Tongling mining area, China. Ecotoxicol. Environ. Saf. 90, 103–111.
Yang, T., Hodson, M.E., 2019. Investigating the use of synthetic humic-like acid as a soil washing treatment for metal contaminated soil. Sci. Total Environ. 647, 290–300.
Yeganeh, M., Afyuni, M., Khoshgoftarmanesh, A.H., Khodakarami, L., Amini, M., Soffyanian, A.R., Schulin, R., 2013. Mapping of human health risks arising from soil nickel and mercury contamination. J. Hazard. Mater. 244–245, 225–239.
Zeng, Q., Liu, Y., Shen, L., Lin, H., Yu, W., Xu, Y., Li, R., Huang, L., 2021. Facile preparation of recyclable magnetic Ni@filter paper composite materials for efficient photocatalytic degradation of methyl orange. J. Colloid Interface Sci. 582, 291–300.
Zhang, Y.J., Ou, J.L., Duan, Z.K., Xing, Z.J., Wang, Y., 2015. Adsorption of Cr (VI) on bamboo bark-based activated carbon in the absence and presence of humic acid. Colloid Surf. A 481, 108–116.
Zou, D.Y., Ma, J., Zou, D., Zhang, H., Diao, R.L., Guo, C.W., 2005. Different from microbial starter and wood vinegar in peat fermentation application effect study. Humic Acid (5), 11–15 (in Chinese).